Cellular/Molecular

Sustained Firing of Cartwheel Cells in the Dorsal Cochlear Nucleus Evokes Endocannabinoid Release and Retrograde Suppression of Parallel Fiber Synapses

Miloslav Sedlacek, Philip W. Tipton, and Stephan D. Brenowitz

Section on Synaptic Transmission, National Institute on Deafness and Other Communication Disorders, National Institutes of Health, Bethesda, Maryland 20892

Neurons in many brain regions release endocannabinoids from their dendrites that act as retrograde signals to transiently suppress neurotransmitter release from presynaptic terminals. Little is known, however, about the physiological mechanisms of short-term endocannabinoid-mediated plasticity under physiological conditions. Here we investigate calcium-dependent endocannabinoid release from cartwheel cells (CWCs) of the mouse dorsal cochlear nucleus (DCN) in the auditory brainstem that provide feedforward inhibition onto DCN principal neurons. We report that sustained action potential firing by CWCs evokes endocannabinoid release in response to submicromolar elevation of dendritic calcium that transiently suppresses their parallel fiber (PF) inputs by >70%. Basal spontaneous CWC firing rates are insufficient to evoke tonic suppression of PF synapses. However, elevating CWC firing rates by stimulating PFs triggers the release of endocannabinoids and heterosynaptic suppression of PF inputs. Spike-evoked suppression by endocannabinoids selectively suppresses excitatory synapses, but glycinergic/GABAergic inputs onto CWCs are not affected. Our findings demonstrate a mechanism of transient plasticity mediated by endocannabinoids that heterosynaptically suppresses subsets of excitatory presynaptic inputs to CWCs that regulates feedforward inhibition of DCN principal neurons and may influence the output of the DCN.

Introduction

In the mammalian brain, endocannabinoid signaling enables neurons to regulate the strength of their inputs in a retrograde manner (Wilson and Nicoll, 2002; Freund et al., 2003; Kano et al., 2009). Depolarization-induced suppression of excitation (DSE) or inhibition (DSI) requires elevation of dendritic calcium and produces widespread release of endocannabinoids that activate presynaptic CB1 receptors, suppressing synaptic strength for tens of seconds (Kreitzer and Regehr, 2001; Ohno-Shosaku et al., 2001; Wilson and Nicoll, 2001). Calcium concentrations of several micromolar are required to evoke DSE and DSI (Wang and Zucker, 2001; Brenowitz and Regehr, 2003; Maejima et al., 2005), suggesting that this phenomenon may not ordinarily occur in healthy neurons. However, sustained firing of sodium spikes (Myoga et al., 2009) or burst firing (Brenowitz et al., 2006) can evoke endocannabinoid release with much lower elevations of calcium, suggesting that endocannabinoids may contribute to short-term synaptic plasticity under physiological conditions.

Received Aug. 9, 2011; revised Sept. 8, 2011; accepted Sept. 14, 2011.

Author contributions: S.D.B. designed research; M.S. and P.W.T. performed research; M.S., P.W.T., and S.D.B. analyzed data; M.S., P.W.T., and S.D.B. wrote the paper.

This work was supported by the National Institute on Deafness and Other Communication Disorders Intramural Research Program. We thank Drs. Jeff Diamond, David Lovinger, Ron Petralia, and Shan He for comments on the manuscript.

Correspondence should be addressed to Dr. Stephan D. Brenowitz, National Institutes of Health, Building 50, Room 4152, 9000 Rockville Pike, Bethesda, MD 20892. E-mail: brenowitzs@nidcd.nih.gov.

DOI:10.1523/JNEUROSCI.4088-11.2011

 0270-6474/11/3115807-11$15.00/0

Endocannabinoid signaling contributes to short-term synaptic plasticity in the dorsal cochlear nucleus (DCN) (Tzounopoulos et al., 2007; Zhao et al., 2009). The DCN integrates auditory and nonauditory information, and has been proposed to play a role in sound localization (Young and Davis, 2002; Oertel and Young, 2004) and filtering of self-generated noise (Shore and Zhou, 2006; Requarth and Sawtell, 2011). Inputs to DCN conveying somatosensory information originate in regions including the dorsal column nuclei (Wright and Ryugo, 1996), spinal trigeminal nucleus (Zhou and Shore, 2004), and trigeminal ganglion (Shore et al., 2000). These inputs excite auditory granule cells, whose parallel fiber (PF) axons form glutamatergic synapses onto fusiform cells—the principal neurons of the DCN—and cartwheel cells (CWCs), glycinergic interneurons that inhibit fusiform cells. Through feedforward inhibition mediated by CWCs, somatosensory input to DCN suppresses spontaneous firing (Davis et al., 1996) and modulates sound-evoked responses (Kanold et al., 2011; Koehler et al., 2011) of fusiform cells. CB1 receptors are expressed on presynaptic terminals of PFs, and depolarization of CWCs evokes DSE of PF EPSCs (Tzounopoulos et al., 2007; Zhao et al., 2009). However, the calcium levels required for DSE are not known, and physiological mechanisms that contribute to endocannabinoid-mediated short-term plasticity at PF–CWC synapses are not well understood.

While CWCs exhibit molecular and physiological similarities to cerebellar Purkinje cells (Mugnaini et al., 1987; Berrebi et al., 1990; Zhang and Oertel, 1993; Manis et al., 1994), one difference is that CWCs express voltage-gated sodium channels in their dendrites. This enables backpropagating action potentials to evoke

dendritic calcium transients (Molitor and Manis, 2003; Roberts et al., 2008) that could contribute to endocannabinoid release. Here we investigated the role of dendritic calcium in endocannabinoid-mediated short-term plasticity at synapses onto CWCs. We find that DSE has a high calcium requirement of several micromolar. However, sustained elevation of dendritic calcium to submicromolar concentrations during action potential trains evokes endocannabinoid release that suppresses PF synapses with no effect on glycinergic inputs. PF activity can elevate CWC firing rates and evoke endocannabinoid release, enabling CWCs to regulate the balance between excitatory and inhibitory inputs to fusiform cells.

Materials and Methods

Slice electrophysiology. All experiments were conducted in accordance with procedures approved by the NIH Animal Care and Use Committee. Recordings were made from coronal brainstem slices (300 μm thick) prepared from P14–P20 ICR and CBA/J mice of either sex. Dissections were performed in an ice-cold, sucrose-based extracellular solution that contained the following (in mM): 75 NaCl, 26 $NaHCO_3$, 75 sucrose, 25 glucose, 2.5 KCl, 1.25 NaH_2PO_4, 7 $MgCl_2$, and 0.5 $CaCl_2$ (~325 mOsm). Slices were then incubated in the same solution for 20 min at 34°C, transferred to saline solution that contained the following (in mM): 125 NaCl, 26 $NaHCO_3$, 25 glucose, 2.5 KCl, 1.25 NaH_2PO_4, 1 $MgCl_2$, and 2 $CaCl_2$ (~315 mOsm) and were incubated for an additional 20 min at 34°C. In some experiments, we performed the dissections at 30–31°C in extracellular solution that contained the following (in mM): 130 NaCl, 20 $NaHCO_3$, 10 glucose, 3 KCl, 1.2 KH_2PO_4, 3 Na-HEPES, 1.3 $MgSO_4$, and 2.4 $CaCl_2$ (~305 mOsm) and incubated the slices in the same solution at 34°C for 45 min. We did not observe any significant differences in results obtained using these two approaches; therefore, we combined the experiments together. All solutions were bubbled with 5% O_2/95% CO_2. For voltage-clamp recordings, glass electrodes (3–5 MΩ) filled with an intracellular solution that contained the following (in mM) were used: 135 $CsMeSO_4$, 15 HEPES, 0.2 EGTA, 1 $MgCl_2$, 15 TEA-Cl, 2 Mg-ATP, 0.3 Na-GTP, 10 Tris-phosphocreatine, and 2 QX-314 [2(triethylamino)-*N*-(2,6-dimethylphenyl)acetamine] (~300 mOsm) and pH adjusted to 7.3 with CsOH. For current-clamp recordings, the intracellular solution contained the following (in mM): 130 $KMeSO_4$, 10 HEPES, 5 NaCl, 0.2 EGTA, 1 $MgCl_2$, 4 Mg-ATP, 0.4 Na-GTP, and 14 Tris-phosphocreatine (~300 mOsm) and pH adjusted to 7.3 with KOH. Recordings of IPSCs were made using the potassium-based intracellular solution to which 20 mM KCl was added, replacing an equimolar amount of $KMeSO_4$, resulting in a chloride reversal potential of ~−40 mV. ACSF was supplemented with 1 μM strychnine and 40 μM picrotoxin to block glycinergic and GABAergic synaptic transmission, with the exception of experiments measuring sIPSCs. Picrotoxin, AM251, U73122, edelfosine, and TTX were from Tocris Cookson. Alexa Fluor 594 hydrazide, Fluo-4FF, and Fluo-5F were from Invitrogen. All other chemicals were purchased from Sigma. All experiments were performed at 34 ± 1°C.

Data acquisition and analysis. Electrophysiology data were filtered at 3 kHz using a MultiClamp 700B amplifier (Molecular Devices), and sampled at 10 kHz. PFs were stimulated with glass electrodes filled with saline and placed in the molecular layer of the DCN. PF EPSCs were evoked with 200 μs current pulses (5–50 μA) delivered by an isolated stimulus unit. In voltage-clamp recordings, cells were held at −60 to −70 mV. In current-clamp recordings, hyperpolarizing current was injected to maintain the CWC membrane potential between −70 and −80 mV and to suppress spontaneous firing. Bridge balance and pipette capacitance neutralization were set and adjusted throughout the experiment. For experiments monitoring effects of spike trains on spontaneous IPSCs (see Fig. 7), the mode of the amplifier was switched between voltage-clamp and current-clamp using an external signal controlled by the data acquisition software. Data were acquired and analyzed using custom routines written in IGOR Pro (WaveMetrics) and MATLAB (MathWorks). Spontaneous IPSCs were detected using a derivative thresholding routine and aligned by their rising phase. Averages are presented as means ± SEM. Parameters of fits to the Hill equation are presented as means ± 95% confidence intervals.

Calcium imaging. Intracellular recording solutions were supplemented with Alexa Fluor 594 hydrazide (20 μM) to visualize the cell morphology and the calcium indicators Fluo-5F (150 μM) or Fluo-4FF (500 μM) as indicated. EGTA was omitted from intracellular solutions during imaging experiments. We used a two-photon laser scanning microscope (2PLSM) with 60×, 0.9 NA objective (Olympus) and a Ti:sapphire pulsed laser (Chameleon; Coherent) tuned to 810 nm for excitation. Fluorescence signals were collected in the epifluorescence and transfluorescence pathways (using a 1.4 NA oil-immersion condenser). Fluorescence signals were separated using a 565 nm dichroic mirror, and green and red fluorescence were collected using 525/50 nm and 629/53 nm bandpass filters, respectively (Semrock). Fluorescence was detected using H7442P and R9110 photomultipliers (Hamamatsu Photonics) for green and red channels, respectively. Imaging and physiology were controlled with custom software written in MATLAB (MathWorks). Calcium transients were measured in line scan mode at 500 Hz across a spine and a parent dendritic shaft of CWCs. Fluorescence signals were converted to calcium concentrations using the equation $[Ca] = K_D^*(R - R_{min})/(R_{max} - R)$, where R is the experimentally measured ratio of green to red fluorescence. The values of R_{min} and R_{max} (Grynkiewicz et al., 1985) were measured with intracellular solutions containing 0 mM Ca/10 mM EGTA and 10 mM Ca, respectively. The K_D values of Fluo-5F and Fluo-4FF used were 0.585 and 8.1 μM, respectively (Yasuda et al., 2004; Brenowitz et al., 2006).

Results

Release of endocannabinoids by DCN CWCs

Previous studies have shown that depolarization of CWCs evokes release of endogenous cannabinoids that transiently suppress synaptic strength at their PF synaptic inputs (Tzounopoulos et al., 2007; Zhao et al., 2009). To further investigate the role of endocannabinoids at PF–CWC synapses and determine the calcium dependence of DSE, whole-cell voltage-clamp recordings were obtained from CWCs, and their identity was confirmed by visualizing the morphology of the cells with fluorescence microscopy (Fig. 1*A*). The protocol for evoking DSE is shown in Figure 1*B*. To quantify DSE, the average amplitudes of the three EPSCs preceding ("pre") and immediately following ("post") a voltage step were measured, and DSE was defined as 1 − (post/pre). DSE evoked by 5 s voltage steps under control conditions was 48.7 ± 3.0% (Fig. 1*B*,*C*; $n = 8$). This suppression was abolished following bath application of the CB1 receptor antagonist AM251 (Fig. 1*B*,*C*; DSE = −0.6 ± 1.3%; $n = 9$). Maximum levels of DSE were obtained with 1 s voltage steps, and no additional suppression was observed with more prolonged depolarization of cartwheel cells (Fig. 1*D*).

Calcium dependence of DSE

High levels of dendritic calcium are required for DSE in cerebellar Purkinje cells (Brenowitz and Regehr, 2003; Maejima et al., 2005), but the calcium requirement for DSE in CWCs is not known. Therefore, we combined synaptic recordings with calcium imaging to determine the relationship between postsynaptic calcium transients and suppression of PF EPSCs. To measure dendritic calcium, CWCs were loaded through the patch pipette with the low-affinity green fluorescent calcium indicator Fluo-4FF (500 μM, $K_D = 8.1$ μM). Since this indicator has very low fluorescence at resting calcium levels, neurons were also loaded with the red fluorophore Alexa Fluor 594 (20 μM) to permit visualization of dendrite and spine morphology (Fig. 2*A*). We used 2PLSM to measure calcium transients evoked in CWC dendrites and spines by voltage steps. Both fluorophores were efficiently excited with a Ti:sapphire laser tuned to 810 nm, and

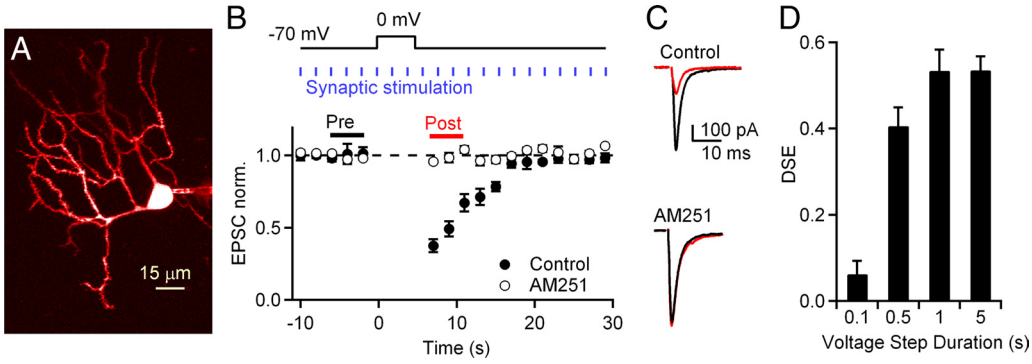

Figure 1. Depolarization of CWCs induces endocannabinoid-mediated suppression of excitatory synaptic transmission at PF to CWC synapses. ***A***, A 2PLSM image of a CWC loaded with Alexa Fluor 594. ***B***, EPSC amplitudes during a representative DSE trial under control conditions and after application of the CB1 receptor antagonist AM251 (5 μM). Top, PFs were stimulated at 0.5 Hz and a 5 s voltage step to 0 mV was used to induce DSE. Bottom, Normalized EPSC amplitudes during DSE trials with 5 s voltage steps plotted under control conditions ($n = 8$) and in AM251 ($n = 9$). ***C***, PF EPSCs (averages of 3 events) at the time points indicated in ***B*** are shown for control conditions (top) and in the presence of AM 251 (bottom) for this representative CWC. ***D***, Voltage steps of 0.1, 0.5, 1, and 5 s were used to determine the relationship between the amount of DSE and the voltage-step duration.

fluorescence emission was separated with a dichroic mirror to allow simultaneous collection of green and red fluorescence. Line scans were performed at 500 Hz across a spine and its neighboring dendrite during voltage-step trials (Fig. 2*A*,*B*), and fluorescence signals were converted to calcium concentrations using ratiometric equations as described in the Materials and Methods.

Our strategy for measuring the calcium dependence of DSE was to determine the relationship between peak levels of dendritic calcium evoked by voltage steps and the amount of suppression of PF EPSCs. However, it was not possible to determine the precise dendritic location of the PF synapses, because extracellular stimulation activated a population of fibers that synapse over a region of the CWC dendritic tree. Calcium levels may reach different levels in different dendritic regions as a result of spatial gradients of ion channel density, changes in dendrite diameter, and the inability to voltage-clamp electrotonically distant regions of the CWC dendrite. Therefore, we measured calcium transients in both proximal and distal CWC dendrites and spines to determine the range of calcium levels reached throughout the dendritic tree during voltage steps (Fig. 2*C*). Proximal regions were selected by locating spines that appeared on proximal dendrites closest to the soma (range, 22–27 μm from the center of the soma; $n = 5$). Distal sites were chosen along the same dendritic branch at tips of dendrites near the pial surface (range, 80–116 μm from the center of the soma measured along the dendritic path; $n = 5$). An example of such an experiment is shown in Figure 2*C* in which calcium transients were measured in a proximal and a distal dendritic location in response to 1 s depolarizations. In a proximal dendrite 25 μm from the soma, calcium reached a plateau of 6.7 μM during the voltage step. In a subsequent trial in the same neuron at a distal site 96 μm from the soma, dendritic calcium reached 6.5 μM (6% lower than at the proximal site). During voltage steps ranging from 0.1 to 5 s, calcium at distal sites reached levels that were 9.4 $\pm$ 3.3% lower than at proximal sites ($n = 5$ neurons, data not shown). In addition, peak levels of calcium in dendritic spines and the neighboring shaft were not significantly different, so in subsequent voltage-clamp experiments we focused on measuring calcium transients in proximal dendritic shafts of CWCs.

To determine the dependence of the amount of DSE on the peak dendritic calcium during voltage steps, we combined synaptic recordings with dendritic calcium imaging in the same neurons. Data from a representative CWC are shown in Figure 2*D*,*E*. In this neuron, a voltage step of 0.1 s elevated calcium to 2.0 μM in the proximal dendrite, but the EPSC was not suppressed. When the voltage step was extended to 0.5 s, peak dendritic calcium reached 5.6 μM and EPSCs were suppressed by 52%. Prolonging the voltage step to 1 and 5 s further elevated calcium and increased DSE to 61 and 65%, respectively. Results from a group of five neurons are summarized in Figure 2*F*,*G*. Maximal suppression of EPSCs was 53.4 $\pm$ 4.8% and was obtained with voltage steps of 1–5 s that produced peak calcium transients of 7.4 $\pm$ 1.0 μM in proximal dendrites and 6.1 $\pm$ 1.1 μM in distal dendrites (Figs. 1*D*, 2*F*).

To obtain a measure of the calcium dependence of DSE in CWCs, we plotted the amount of DSE for each trial against peak dendritic calcium measured in proximal regions of CWC dendrites (Fig. 2*G*). A fit of the data points to the Hill equation indicated that the dendritic calcium concentration producing half-maximal DSE was 3.9 μM and the Hill coefficient was 5.7. Because calcium levels in distal regions of CWC dendrites are slightly lower, our results demonstrate a high calcium requirement for DSE in the range of 3.6–3.9 μM. Also, because of the steep cooperativity, brief calcium transients with peaks less than ~2 μM are not effective in evoking endocannabinoid release.

Dendritic calcium transients during spontaneous CWC activity

Because CWCs fire spontaneously *in vivo* (Davis and Young, 1997; Ding and Voigt, 1997; Portfors and Roberts, 2007) and in brain slices (Zhang and Oertel, 1993; Kim and Trussell, 2007), we investigated whether action potential backpropagation during sustained firing of CWCs could elevate dendritic calcium and evoke endocannabinoid release. Spontaneous firing rates of CWCs in slices measured with cell-attached recordings (Fig. 3*A*, top) ranged from 12 to 26 Hz (mean 18 $\pm$ 2; $n = 10$). In whole-cell current-clamp recordings, CWCs held with zero bias current were spontaneously active at 21.3 $\pm$ 0.8 Hz (range, 19.5–23.9 Hz; $n = 6$) (Fig. 3*A*, bottom). Although in some cases complex spikes were observed, in subsequent experiments we focused on the role of simple sodium spikes in producing dendritic calcium transients and retrograde inhibition, and cells firing complex spikes at rates >1 Hz were excluded from our analysis.

Action potentials in CWCs can backpropagate and evoke dendritic calcium transients (Molitor and Manis, 2003; Roberts et al., 2008). We measured calcium transients in CWC dendrites and spines at proximal and distal locations to confirm that calcium transients propagate throughout the dendritic tree. In response

to single action potentials triggered with brief current injections (2 ms; 1–2 nA), calcium transients were always observed in both proximal and distal dendrites and spines of CWCs (Fig. 3*B*), indicating that calcium levels throughout CWC dendrites become elevated during ongoing spontaneous firing. To determine the relationship between CWC firing rates and dendritic calcium levels during spike trains, we measured dendritic calcium during spike trains of different frequencies that were obtained by varying the amplitude of current injections. Results from a representative CWC are shown in Figure 3*C* (left). In response to a series of current steps that ranged from 100 to 500 pA, dendritic calcium levels reached a plateau level that was dependent on the CWC firing frequency. Data from multiple trials from six CWCs were binned by spike rate, indicating that dendritic calcium levels progressively increase with firing rates in CWCs (Fig. 3*C*, right). In addition, the differences in calcium levels between spines and neighboring dendritic shafts following single spikes in proximal dendritic regions (Fig. 3*B*) were not observed during trains of action potentials. These results indicate that during spontaneous firing dendritic calcium increases to a plateau level of several hundred nanomolar, suggesting that prolonged spiking could evoke endocannabinoid release from CWC dendrites and produce retrograde suppression of PF inputs.

Repetitive firing evokes endocannabinoid release and suppression of PF synapses

To test whether sustained firing by CWCs evokes endocannabinoid release, we measured PF EPSPs before and after spike trains of 15 s duration. Current injection amplitudes were adjusted to generate sustained firing of simple spikes throughout the 15 s trial, and PF EPSPs were evoked at 0.5 Hz before and after the spike train. A representative trial is shown in Figure 4*A* in which the CWC fired for 15 s at a mean rate of 34.5 Hz. Suppression of EPSPs (calculated as the ratio of the mean of three EPSPs evoked after vs before the spike train) was 79%, and returned to baseline levels over ~20 s (Fig. 4*B*). We next examined the effects of varying the duration of CWC firing on PF suppression by monitoring EPSP amplitudes before and after action potential trains of 1, 5, and 15 s (Fig. 4*C*). For the five neurons tested, mean firing rates during the spike train were 42 ± 2 Hz. After 1 s of firing, no suppression of PF EPSP amplitudes was observed ($p > 0.05$, *t* test). Following 5 and 15 s spike trains, the amplitudes of EPSPs evoked 1 s after the spike train were suppressed by 38.1 ± 8.8% ($p < 0.01$, *t* test) and 79.6 ± 3.5% ($p < 0.01$, *t* test), respectively.

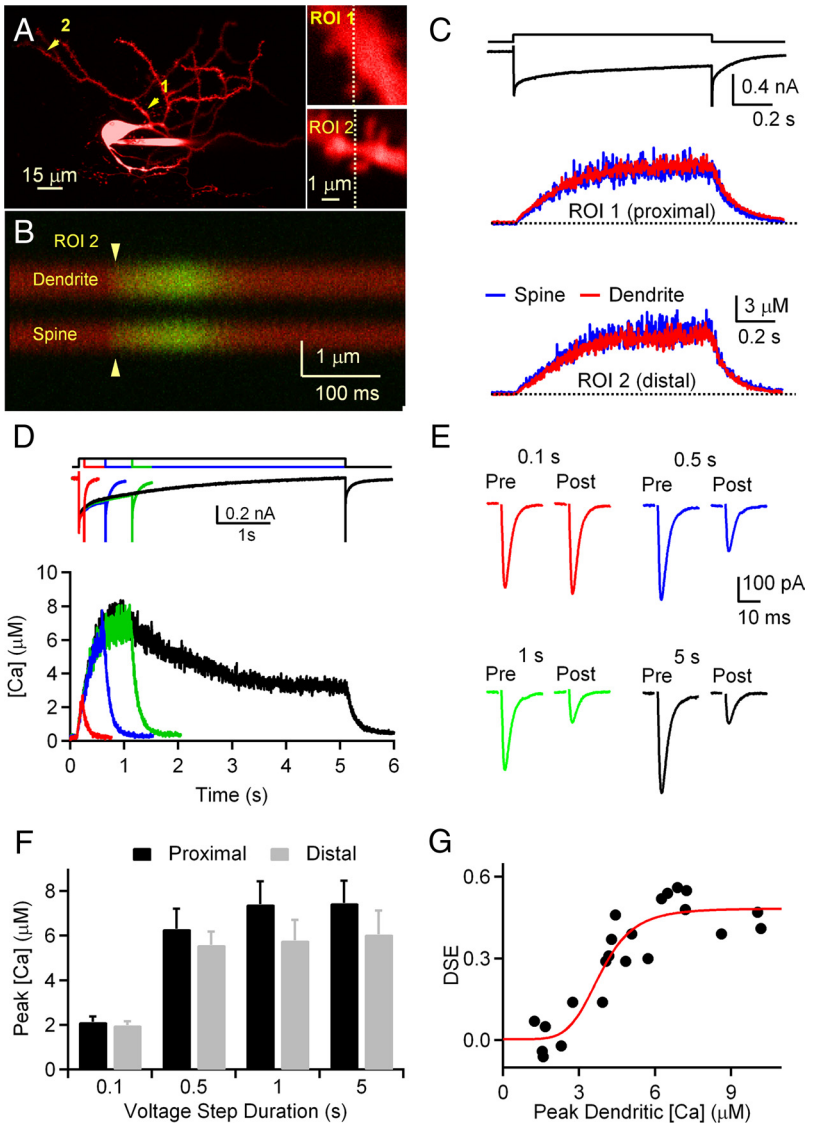

Figure 2. Calcium requirements for CWC DSE. ***A***, Left, Image of the CWC loaded with Alexa Fluor 594. Right, Enlarged views of proximal and distal dendritic regions of interest (ROIs) indicated in the left panel by 1 and 2, respectively. Line scans across the spine and neighboring dendrite were obtained at the position indicated by dashed lines during the depolarizing voltage step. ***B***, Fluorescence collected during line scans at ROI 2 indicated by the dashed line in ***A***. The increased green fluorescence indicates increased intracellular calcium in both spine and dendritic shaft, whereas the level of red (calcium-insensitive) fluorescence remains unchanged. ***C***, Voltage steps from the holding potential of −70 to 0 mV for 1 s produced an inward current that evoked calcium transients in spines (blue traces) and neighboring dendritic shafts (red traces) in proximal (ROI 1 in ***A***) and distal (ROI 2 in ***A***) regions of a CWC. The ratio of green fluorescence to red fluorescence (ΔG/R) was converted to [Ca] as described in the Materials and Methods. ***D***, Calcium transients in CWC dendrites and spines during prolonged depolarizations. Top, Voltage steps of 0.1, 0.5, 1, and 5 s, and corresponding whole-cell currents from a representative CWC are shown. Bottom, Calcium transients in proximal dendritic shaft during voltage steps shown above from the same cell. ***E***, Suppression of EPSC amplitudes following voltage steps of indicated durations. Traces represent averages of three EPSCs preceding (Pre) and following (Post) each voltage step. Data in ***D*** and ***E*** are from the same cell. ***F***, Peak intracellular calcium in proximal and distal dendrites of CWCS during voltage steps of 0.1–5 s (n = 5 cells). ***G***, Dependence of PF EPSC suppression on changes in dendritic [Ca]. DSE is plotted versus peak [Ca] measured from a proximal dendritic location. Each point represents a single trial (n = 5 cells). A fit of the data to the Hill equation (in red) indicates that 3.9 μM calcium was required for half-maximal DSE.

To test the role of endocannabinoid release in PF suppression, we repeated the 15 s spike trains in the presence of the CB1 receptor antagonist AM251 (Fig. 4*D*,*E*). As demonstrated in the group data (Fig. 4*E*), EPSP suppression by the 15 s spike train was reduced from 75.5 ± 2.8% (control; n = 4) to 9.6 ± 3.7% (AM251; n = 4). The amplitudes of EPSPs evoked ≥3 s after the end of a 15 s spike train were not significantly different from the prestimulus baseline ($p > 0.05$, *t* test; n = 4). However, the EPSP

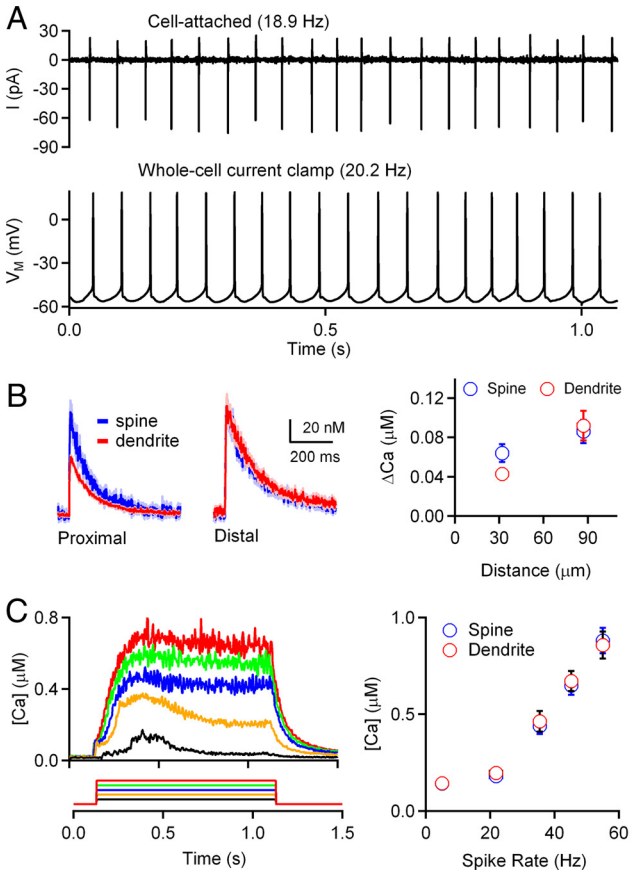

Figure 3. Sodium action potentials backpropagate into the CWC dendrites and elevate intracellular calcium. ***A***, CWCs are spontaneously active. Top, Cell-attached recording of action potentials in tonic firing mode, performed in voltage-clamp mode with pipettes containing standard ACSF. Bottom, In whole-cell current-clamp recordings, CWCs are spontaneously active when no hyperpolarizing current is applied to the cell. A representative example of a CWC firing spontaneously in tonic mode is shown. ***B***, Left, Backpropagation of single sodium action potentials evoked by short somatic current injections (2 ms; 1–2 nA) generate calcium transients in CWC dendrites and spines. Calcium transients in proximal (16–44 μm from soma) and distal (76–115 μm from soma) spines and dendritic shafts during a single sodium spike were compared. Data are shown as mean (line) ± SE (shaded region) from one cell. Right, Peak [Ca] in proximal and distal dendritic spines and shafts was plotted as a function of distance from the CWC soma ($n = 5$ cells). ***C***, Left, Representative traces showing calcium transients in dendritic shaft during 1 s current injections (100–500 pA in 100 pA increments). Each trace represents the average of 5 trials for each current injection acquired from one cell. Right, Mean dendritic calcium levels during 1 s spike trains were binned according to CWC firing rates ($n = 6$).

evoked 1 s after the termination of action potential firing was suppressed by 22 ± 7% ($p < 0.05$, t test; $n = 4$) relative to EPSP amplitudes before the spike train. Suppression of the first EPSP in the presence of AM251 could arise from a variety of mechanisms, including incomplete blockade of CB1 receptors, release of an additional retrograde messenger, or alteration in dendritic filtering following 15 s action potential trains. In contrast, under control conditions, PF suppression was substantially greater and the amplitudes of EPSPs remained significantly suppressed for >20 s after the spike train. The results indicate that sustained firing by CWCs evokes endocannabinoid release that causes prolonged suppression of PF inputs.

Endocannabinoid production can be greatly facilitated by synergistic interactions between postsynaptic calcium and metabotropic receptors coupled to $G_{q/11}$ proteins that activate phospholipase C (PLC) (Maejima et al., 2001; Varma et al., 2001; Ohno-Shosaku et al., 2002; Brown et al., 2003; Brenowitz and Regehr, 2005). CWCs express multiple $G_{q/11}$-coupled metabotropic receptors including mGluR1 (Petralia et al., 1996; Wright et al., 1996; Molitor and Manis, 1997; Fujino and Oertel, 2003) and M1/M3 mAchRs (Chen et al., 1995). To test whether PLC-coupled metabotropic receptors contribute to spike-evoked endocannabinoid release, we performed experiments using the PLC inhibitors U73122 (5 μM) and edelfosine (10 μM). Slices were incubated in either U73122 or edelfosine for at least 30 min, and physiological recordings were performed in the continued presence of the drug. Suppression of PF EPSPs during 15 s spike trains was not affected by pharmacological block of PLC with either inhibitor (Fig. 5*A*,*B*).

Recent studies have shown that the endocannabinoid 2-arachidonylglycerol (2-AG) is responsible for DSE, DSI, and PLC-dependent endocannabinoid release in several brain regions (Zhao et al., 2009; Gao et al., 2010; Tanimura et al., 2010). However, the identity of the endocannabinoid released during sustained firing of CWCs is not known. Therefore, to further explore the mechanism of endocannabinoid release from CWCs during spike trains we examined the effects of tetrahydrolipostatin (THL), an inhibitor of DAG lipase, the major biosynthetic enzyme for 2-AG. We found that application of THL (10 μM) strongly reduced suppression of EPSPs evoked by 15 s tonic firing of CWCs (Fig. 5*C*,*D*) (17 ± 0.4% suppression in THL vs 86 ± 4% suppression under control conditions; $n = 4$). Consistent with a recent study (Zhao et al., 2009), we also observed that THL greatly reduces DSE at PF–CWC synapses (Fig. 5*E*,*F*) (14 ± 2% suppression in THL vs 69 ± 5% under control conditions; $n = 3$). Together, our results indicate that $G_{q/11}$-coupled metabotropic receptors do not contribute to spike-evoked endocannabinoid release, suggesting that elevation of dendritic calcium evoked by backpropagating action potentials or direct depolarization causes synthesis and release of 2-AG from CWCs that results in PF suppression.

Calcium dependence of spiking-evoked PF suppression

Based on our findings that dendritic calcium levels are dependent on CWC firing rates (Fig. 3*C*), we next examined the calcium dependence of spiking-evoked PF suppression in CWCs by combining physiological recordings of EPSPs with calcium measurements in CWC dendrites. In these experiments, we applied current injections (200–500 pA) during 15 s spike trains to vary the CWC firing rate between 5 and 50 Hz. As in the case of DSE experiments, we first compared calcium transients in proximal and distal regions of the CWC dendrite to determine the range of postsynaptic calcium levels at PF synapses throughout the CWC. Despite the differences in peak calcium levels in response to a single action potential (Fig. 3*B*), calcium levels were not different in proximal and distal dendrites during 15 s spike trains (Fig. 6*A*,*B*). Moreover, calcium levels in spines and the parent dendrite were not different in either proximal or distal regions (Fig. 6*A*). Therefore, in the following experiments to determine the calcium dependence of spiking-evoked PF suppression by CWCs we focused on measuring calcium transients in dendritic shafts.

Our experimental approach for measuring the relationship between dendritic calcium and suppression of PF EPSPs is illustrated in Figure 6*C*,*D* for a representative neuron. Dendritic calcium was measured during 1 s spike trains at 5–50 Hz. In this neuron the range of action potential firing rates raised dendritic calcium to levels that did not exceed 1 μM (Fig. 6*C*) yet produced strong suppression of PF EPSPs (Fig. 6*D*). Calcium levels were dependent on CWC firing rates (Fig. 6*E*) and there was a clear trend toward greater amounts of PF suppression with higher fir-

ing rates (Fig. 6*F*). The results indicate that PF EPSPs are suppressed by >50% with submicromolar levels of calcium. This analysis was repeated in a group of nine neurons, and the data were fitted to the Hill equation (Fig. 6*G*,*H*). The parameters of the fit indicated that half-maximal suppression of EPSPs occurred at mean dendritic calcium levels of 0.40 ± 0.07 μM. Compared with DSE, which was half-maximal at 3.9 μM calcium (Fig. 2*G*), this reflects an ~10-fold increase in calcium sensitivity. Thus, submicromolar elevation of dendritic calcium that occurs under conditions where CWC firing rates exceed ~25 Hz for 15 s causes strong suppression of PF synapses mediated by retrograde endocannabinoid signaling.

If the same calcium-dependent signaling pathway is responsible for both DSE and spike-evoked PF suppression in CWCs, it is possible that the long duration of the low-level calcium signal during spike trains compensates for the lower peak requirement compared with DSE. To examine this possibility, we calculated the integral of the calcium transient for experiments in which DSE (Fig. 2*G*) and spike-evoked PF suppression (Fig. 6*G*) were measured (Fig. 6*H*). The integrated calcium transient is proportional to the total calcium influx evoked by either voltage steps or spike trains and can be directly compared, because the same concentration of calcium indicator was used for both voltage-clamp and current-clamp experiments (Neher and Augustine, 1992; Schneggenburger et al., 1993). This analysis indicates that although calcium levels driving endocannabinoid release during CWC spike trains are ~10-fold lower than during DSE trials, a larger total calcium influx is required to obtain a given amount of PF suppression during a spike train compared with a DSE trial.

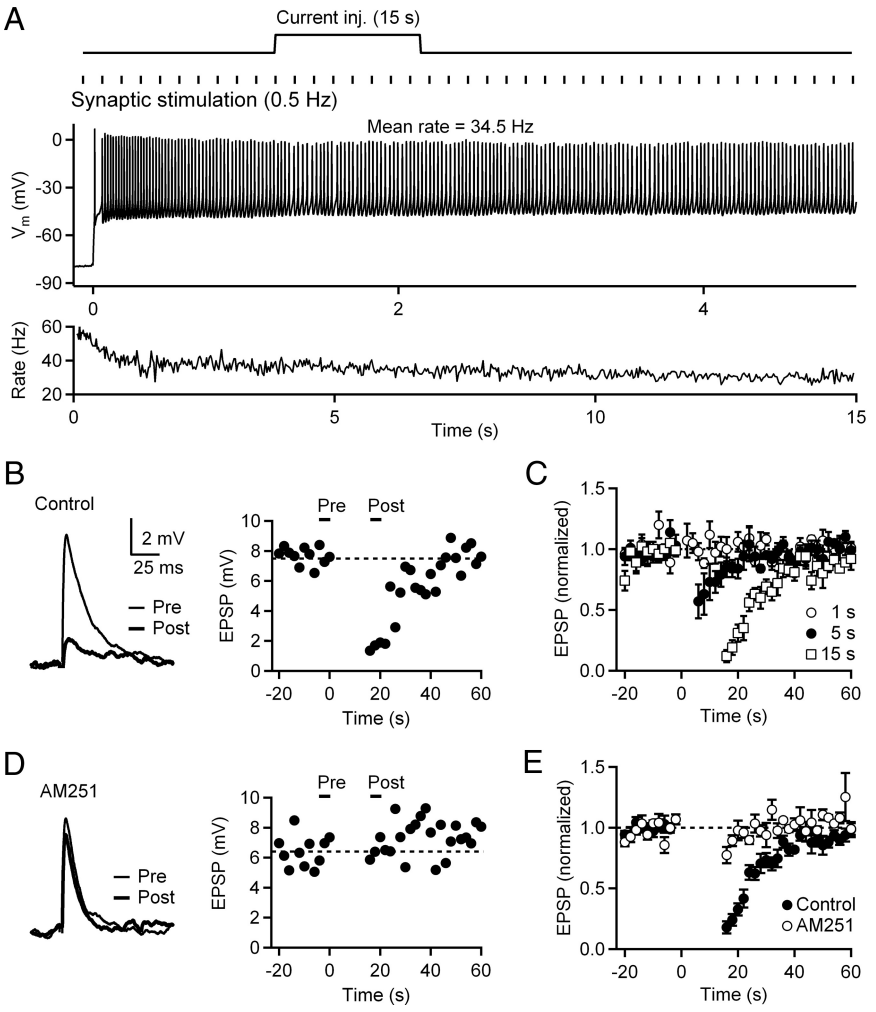

Figure 4. Suppression of PF synapses following sustained firing of CWCs requires endocannabinoid release. ***A***, Top, Schematic of the experimental protocol. PF EPSPs were monitored with 0.5 Hz stimulation in CWCs before and after spike trains evoked by somatic current injections of 1–15 s. Bottom, In a representative CWC, a 15 s current injection (300 pA) evoked a train of action potentials with a mean rate of 34.5 Hz. ***B***, Left, EPSPs (average of 3 consecutive responses) before (Pre) and after (Post) the spike train (same trial as in ***A***). Right, Time course of EPSPs during a trial in which the 15 s spike train began at $t = 0$. ***C***, Normalized EPSP amplitudes during trials of 1, 5, and 15 s of CWC tonic firing ($n = 5$ cells). ***D***, EPSPs recorded in the presence of AM251 before and after a 15 s spike train. Same neuron as ***A*** and ***B***. ***E***, Normalized EPSP amplitudes in control conditions and in the presence of AM251 ($n = 5$).

Endocannabinoids released from CWCs during sustained tonic firing do not suppress inhibitory synapses to CWCs

In addition to glutamatergic PF synaptic inputs, CWCs receive glycinergic and GABAergic inputs from other CWCs and superficial stellate cells (Zhang and Oertel, 1993; Davis and Young, 2000; Roberts et al., 2008). Therefore, we tested the possibility that endocannabinoids released by CWC dendrites during spike trains also suppress these inhibitory synapses. sIPSCs were recorded from voltage-clamped CWCs at a holding potential of −70 mV in extracellular solution supplemented with DNQX (10 μM) to block AMPA receptors. The intracellular concentrations of chloride ions were adjusted so that the reversal potential for chloride was ~−40 mV. Synaptic currents recorded under these conditions were confirmed to be glycinergic/GABAergic as all events could be completely blocked by strychnine (1 μM) and picrotoxin (40 μM) (Fig. 7*A*). sIPSCs were also confirmed to arise from presynaptic spiking because they were eliminated by application of TTX (0.5 μM) (Fig. 7*B*). To test for suppression of sIPSCs by CWC spiking, sIPSCs were recorded in voltage-clamp for 20 s before the amplifier was switched to current-clamp mode to deliver a 15 s current injection. After termination of CWC firing, the amplifier mode was switched back to voltage-clamp and sIPSCs were recorded for 40 s. A representative example of this protocol is shown in Figure 7*C* in which the CWC fired in tonic mode for 15 s at a rate of 39.2 Hz. When sIPSCs were collected and averaged over a 5 s period immediately before and after the spike train, no change was observed in the sIPSC amplitude (Fig. 7*C*). For the five neurons tested (Fig. 7*D*), the average firing rates were 36 ± 3 Hz, a range sufficient to evoke endocannabinoid release and significant suppression of PF synapses (Figs. 4–6). Individual events were collected, binned in 1 s intervals, and sIPSC amplitudes were averaged and plotted for each 1 s interval. Figure 7*D* shows that sustained firing of CWCs had no effect on sIPSC amplitudes.

PF excitation elevates CWCs firing rates and evokes endocannabinoid release

We next tested whether the ongoing spontaneous activity of CWCs produces tonic release of endocannabinoids by compar-

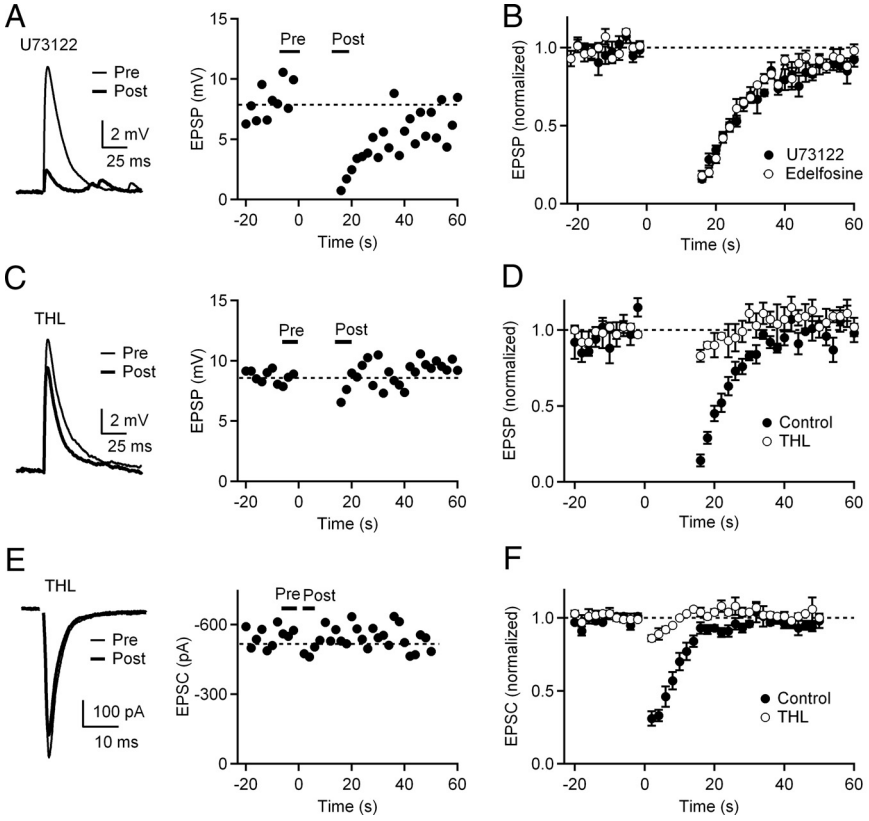

Figure 5. Suppression of PF synapses following sustained firing of CWCs is independent of PLC pathway activation. ***A***, Left, EPSPs recorded in the presence of the PLC inhibitor U73122 before and after a 15 s spike train. Right, Time course of EPSPs recorded in the presence of U73122. ***B***, Normalized EPSPs in the presence of U73122 ($n = 5$) and another PLC inhibitor edelfosine ($n = 5$ cells) during trials consisting of 15 s CWC spike trains. ***C***, 2-AG is released from CWC dendrites during sustained firing. Left, EPSPs recorded in the presence of DAG lipase inhibitor THL before and after a 15 s spike train. Right, Time course of EPSPs recorded in the presence of THL. ***D***, Normalized EPSP amplitudes in control conditions and in the presence of THL ($n = 4$ cells). ***E***, 2-AG is released from CWC dendrites during depolarization. Left, EPSCs recorded in the presence of DAG lipase inhibitor THL before and after 1 s depolarization. Right, Time course of EPSCs recorded in the presence of THL. ***F***, Normalized EPSC amplitudes in control conditions and in the presence of THL ($n = 3$ cells).

ing PF EPSPs before and after a 15 s period in which the CWC fired spontaneously with a bias current of 0 pA (Fig. 8*A*). During the spontaneous firing period, CWCs fired almost exclusively simple spikes at 21.3 ± 0.8 Hz ($n = 6$). PF EPSPs were not suppressed by this spontaneous firing (EPSP amplitudes were 100 ± 9.2% relative to prefiring amplitudes; $n = 6$), indicating that spontaneous CWC firing rates are not sufficiently high to produce tonic release of endocannabinoids.

One mechanism that could increase CWC firing rates and evoke endocannabinoid release is excitatory input from PFs. Therefore, we performed a series of experiments to examine the role of PF excitation in elevating CWC firing rates and causing suppression of PF synapses through release of endocannabinoids from CWCs. Stimulation of PF inputs at 10 Hz for 15 s while maintaining the CWC at a hyperpolarized membrane potential resulted in strong post-tetanic potentiation (PTP) of PF EPSPs (Fig. 8*B*) that decayed over 20–30 s. We next combined 10 Hz PF stimulation with a current injection that maintained the CWC at a holding current of 0 pA (Fig. 8*C*). Despite increasing CWC firing rates to 28.6 ± 2.0 Hz ($n = 6$), PF EPSPs remained strongly potentiated (209 ± 23% relative to prefiring amplitudes; $n = 6$). When this protocol was repeated in the presence of AM251, the amplitudes of PF EPSPs showed only a slight enhancement (Fig. 8*F*) (214 ± 23% relative to preconditioning amplitudes; $p > 0.05$; $n = 4$). These results indicate that any potential effect of endocannabinoid release from the CWC on PF EPSP amplitudes was obscured by the strong potentiation of EPSPs following sustained 10 Hz stimulation.

Therefore, to test for global endocannabinoid release during elevated rates of CWC firing, we performed experiments in which a second stimulus electrode placed in the molecular layer of the DCN was used to activate an independent set of PF inputs to the postsynaptic CWC (Fig. 8*D*). The independence of the two PF pathways was tested by demonstrating the absence of paired-pulse facilitation when alternate pathways were stimulated at 20–50 ms intervals (Brown et al., 2003; Tzounopoulos et al., 2007). In these experiments, we monitored the amplitudes of EPSPs evoked by stimulation of PF pathway 1 before and after a 15 s conditioning stimulus during which the second pathway was activated at 10 Hz during the 15 s period of spontaneous CWC firing. Stimulation of PF pathway 2 increased the firing rates of CWCs from 21.3 ± 0.8 Hz to 29.7 ± 2.1 Hz (Fig. 8*E*; $n = 6$). Following this stimulus protocol, PF EPSPs from pathway 1 were suppressed to 57.3 ± 4.0% (Fig. 8*D*,*F*) ($n = 6$ neurons, 12 pathways) of their preconditioning amplitudes. In each neuron, the ability of each PF pathway to suppress the other was reciprocally tested. This suppression of PF EPSPs was abolished in the presence of AM251 (Fig. 8*F*) (101.7 ± 10.1% relative to amplitudes; $n = 4$). These results demonstrate that PF stimulation can elevate the CWC firing rate and cause global release of endocannabinoids. This form of endocannabinoid-mediated synaptic plasticity is heterosynaptic in nature because it is restricted to the population of PF inputs that are not repetitively activated during the conditioning stimulus. Under these conditions, highly active synapses that increase CWC firing rates became potentiated, whereas synaptic inputs that were inactive exhibit short-term suppression that recovered over 10–15 s as a result of endocannabinoid release from the CWC.

Discussion

Here we investigated the role of calcium-dependent endocannabinoid release in transient suppression of synaptic inputs onto CWCs of the DCN. We find that calcium levels of ~4 μM are required for half-maximal DSE at PF synapses. However, prolonged calcium elevations during CWC firing reduces the calcium requirement for endocannabinoid release by 10-fold such that submicromolar elevations of dendritic calcium cause suppression of PF EPSP amplitudes by >70%. Spiking-evoked endocannabinoid release does not require activation of PLC, but it requires activation of DAG lipase, suggesting that elevation of dendritic calcium produced by action potential backpropagation causes release of the endocannabinoid 2-AG from CWC dendrites. Although basal rates of spontaneous CWC activity (~20 Hz) are insuf-

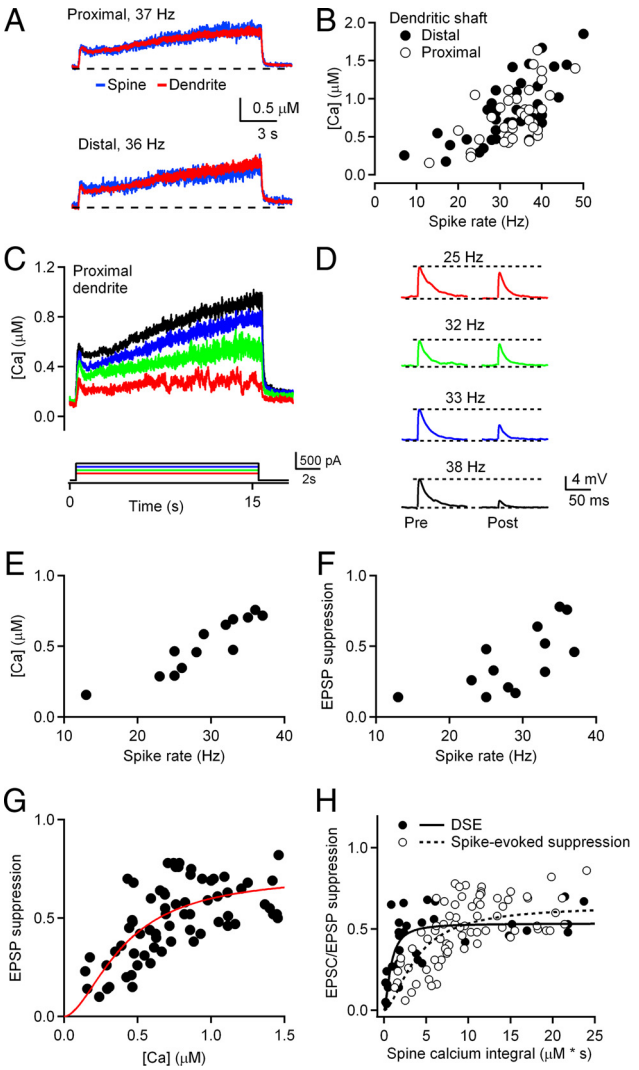

Figure 6. Submicromolar elevation of dendritic calcium in CWCs during tonic spiking evokes endocannabinoid release and suppression of PF synapses. ***A***, Calcium transients in proximal (top) and distal (bottom) dendrite of a representative CWC during a 15 s spike train. ***B***, Summary plot showing the relationship between mean postsynaptic calcium concentration and firing rate during 15 s of CWC spiking for proximal and distal dendrites. Each data point represents one trial ($n = 9$ cells). ***C***, Calcium transients measured in the proximal dendrite of a CWC during 15 s of tonic firing evoked by current injections of 200–500 pA in 100 pA increments. Traces are single trials from the same cell. ***D***, EPSPs before and after spike trains evoked during trials shown in ***C***. Traces in ***C*** and ***D*** represent recordings from the same cell. Color coding of EPSPs in ***D*** corresponds to color coding of calcium transients in ***C***. ***E***, Relationship between CWC firing rates and mean dendritic calcium levels for 15 s current injections of 200–500 pA. ***F***, Relationship between EPSP suppression and mean CWC firing rate during 15 s of spiking. ***G***, Summary data of the dependence of EPSP amplitude suppression on the calcium increase in CWC dendrites. The solid line represents a fit of the Hill equation to the data ($n = 9$ cells). Parameters of this fit yielded a maximum EPSP suppression of 72 ± 9%, which was half-maximal at 0.40 ± 0.07 μM calcium. ***H***, Calcium integral plots for CWC spines showing the summary data of the suppression of EPSCs (voltage-clamp; DSE; $n = 5$ neurons), and EPSPs (current-clamp; spike-evoked suppression; $n = 9$ neurons), respectively. Fits using the Hill equation of both DSE (solid line) and spike-evoked suppression (dashed line) are shown. Maximal suppression under the two conditions were similar (53.4 ± 4.7% for DSE vs 64.2 ± 14.9% for spike-evoked suppression), but there was more than a fourfold difference in the spine calcium integral required for half-maximal suppression (0.79 ± 0.22 μM*s for DSE vs 3.8 ± 1.6 μM*s for spike-evoked suppression).

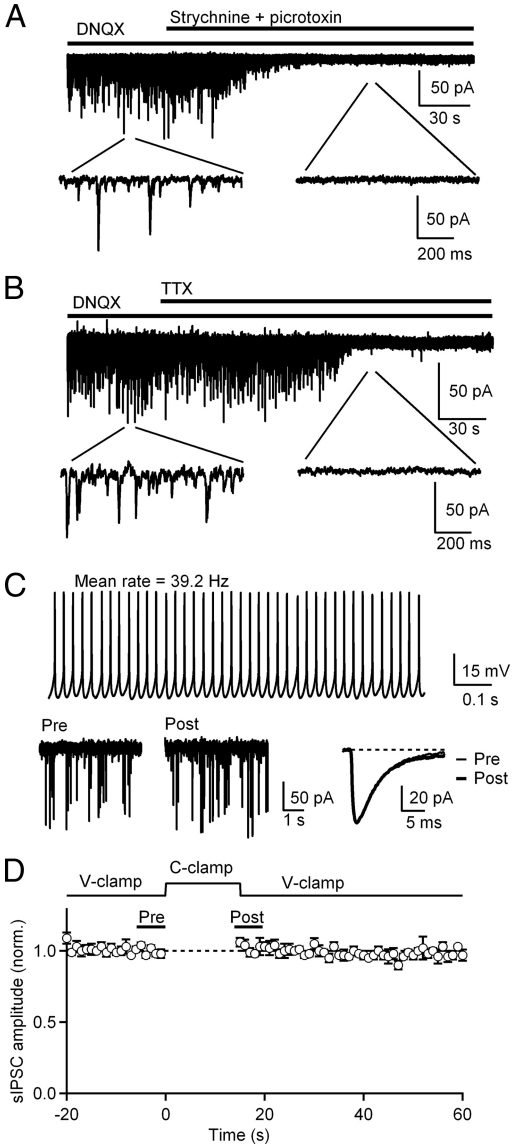

Figure 7. Endocannabinoids released from CWCs during sustained firing do not suppress inhibitory cartwheel or stellate cell inputs. ***A***, sIPSCs were recorded in voltage-clamp at −70 mV ($E_{Cl} = \sim -40$ mV) in continuous presence of DNQX (10 μM). Complete blockade of all events with strychnine (1 μM) and picrotoxin (40 μM) confirmed the glycinergic/GABAergic nature of postsynaptic currents ($n = 5$ cells). ***B***, Bath application of TTX (0.5 μM) blocked spontaneous IPSCs ($n = 5$ cells). ***C***, Top, In a representative CWC, a 15 s current injection-evoked tonic firing at a mean rate of 39.2 Hz (1 s of the trace is shown). Bottom, sIPSCs recorded 5 s before (Pre) and after (Post) the current injection (same neuron as ***B***). Events were averaged before and after CWC firing. ***D***, Top, Experimental protocol for measuring suppression of sIPSCs by CWC spike trains. After 20 s of sIPSC recording in voltage-clamp, the amplifier mode was switched to current-clamp for 15 s to evoke firing in CWC and then switched back to voltage-clamp to record the sIPSCs for 40 s. Bottom, Normalized sIPSC amplitudes before and after 15 s of CWC tonic firing. Individual sIPSCs were collected and binned, and sIPSC amplitudes in 1 s intervals were averaged and plotted ($n = 5$ cells).

ficient to cause suppression of PF synapses, elevating CWC firing rates by stimulation of PFs triggers endocannabinoid-mediated PF suppression in a pathway-specific and heterosynaptic manner. Glycinergic/GABAergic inputs onto CWCs do not exhibit spike-mediated suppression. Our findings demonstrate a novel form of heterosynaptic plasticity mediated by endocannabinoids that selectively suppress subsets of PF inputs to CWCs and may thereby influence the output of the DCN.

Calcium-dependent mechanisms of endocannabinoid release

Consistent with previous studies (Wang and Zucker, 2001; Brenowitz and Regehr, 2003; Maejima et al., 2005), we find that DSE in CWCs requires large elevations of dendritic calcium to several

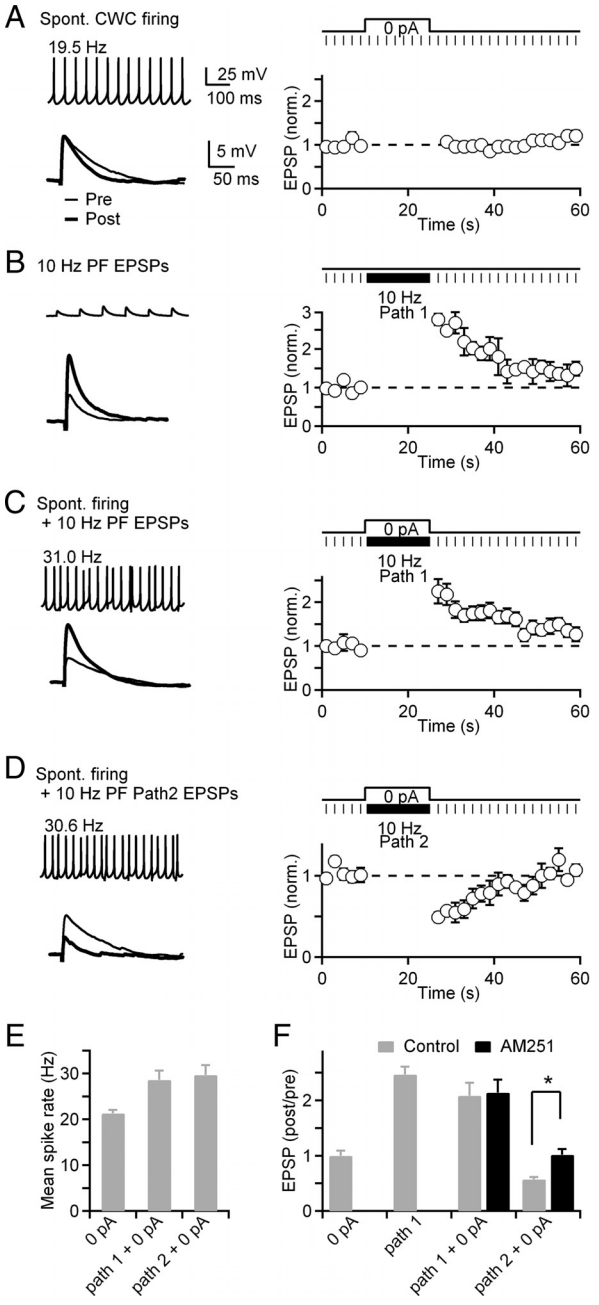

Figure 8. Pathway-specific endocannabinoid release evoked by combined PF stimulation and CWC spontaneous firing. Two stimulus electrodes were used to activate independent populations of PF synapses (paths 1 and 2) onto a postsynaptic CWC. Data from the same representative neuron are shown in the left column of ***A–D*** and pooled data from 6 neurons is shown in the right column. ***A***, EPSPs were monitored before and after the CWC was allowed to fire spontaneously (0 pA bias current) for 15 s. Mean firing rates during the 15 s trial were 21.3 ± 0.8 Hz. Three EPSPs before (Pre) and 3 EPSPs after (Post) 15 s of spontaneous CWC firing were averaged. After spontaneous firing, EPSPs were 100 ± 9.2% of preconditioning amplitudes ($n = 6$). ***B***, Trials in which PF pathway 1 was activated at 10 Hz for 15 s while the cell was silenced by injecting hyperpolarizing current. PF EPSPs were potentiated to 247 ± 14% of their preconditioning amplitude following 10 Hz stimulation ($n = 6$). ***C***, Activation of PF pathway 1 at 10 Hz was combined with a 15 s period of spontaneous CWC firing (at 0 pA bias current). CWC firing rates increased to 28.6 ± 2.0 Hz, and PF EPSP amplitudes were potentiated to 209 ± 23% of their preconditioning amplitude ($n = 6$). ***D***, Trials in which an independent PF pathway (Path 2) was activated at 10 Hz throughout the 15 s period of spontaneous CWC firing. Firing rates of the CWC were increased to 29.2 ± 2.1 Hz. After this conditioning protocol, PF EPSPs evoked in pathway 1 were suppressed to 57.3 ± 4.0% of their preconditioning amplitude. ***E***, Mean CWC firing rates during stimulus protocols shown in ***A***, ***C***, and ***D***. ***F***, Normalized amplitudes of EPSPs evoked in pathway 1 under control conditions ($n = 6$, gray) and in the presence of AM251 ($n = 4$, black) for the different conditioning protocols.

micromolar. Because of the cooperativity between postsynaptic calcium and DSE indicated by the large Hill coefficient, small calcium transients are unable to evoke endocannabinoid release. It is likely that calcium levels sufficient to evoke DSE may occur only under very high activity levels or pathological conditions.

The high calcium requirement for DSE at PF–CWC synapses prompted us to investigate mechanisms that could evoke endocannabinoid release under more physiological conditions. CWCs exhibit spontaneous activity both *in vivo* and in brain slices, and their firing rates can exceed 100 Hz in response to both auditory and somatosensory stimulation (Davis and Young, 1997; Ding and Voigt, 1997). Since backpropagation of action potentials causes elevation of dendritic calcium, we examined the effects of simple spike trains on PF EPSPs and found that spike trains of 5–15 s produced significant amplitude suppression that is dependent on CB1 receptor activation. Moreover, amplitude suppression is not affected by PLC inhibitors, suggesting that spike-evoked suppression of PF EPSPs is dependent solely on elevation of dendritic calcium caused by action potential backpropagation.

Consistent with recent studies indicating that 2-AG is responsible for the endogenous cannabinoid released from neurons in response to elevated calcium (Gao et al., 2010; Tanimura et al., 2010), we found that inhibition of DAG lipase prevented both DSE and spike-evoked endocannabinoid release from CWCs. Despite the common requirement for DAG lipase activity, however, endocannabinoid release from CWCs during trains of action potentials was evoked by elevation of dendritic calcium levels that were ~10-fold lower than required for DSE. One explanation for this difference is that the longer duration of calcium elevation during spike trains compensates for the lower calcium requirement. However, a comparison of the calcium integral for both DSE and spike-evoked PF suppression indicates that greater total calcium influx is required for spike-evoked PF suppression. This suggests the possibility that distinct cellular mechanisms may be responsible for production of DAG: one with high calcium affinity and slow kinetics and another with lower affinity and faster kinetics. Another explanation is that DSE requires less total calcium influx because rapid release of endocannabinoids could saturate uptake and degradation mechanisms and increase CB1 receptor activation. However, measurement of suppression of synaptic responses does not provide a linear readout of endocannabinoid production, making it difficult to distinguish among these mechanisms.

CWCs can fire both simple and complex spikes (Zhang and Oertel, 1993; Manis et al., 1994; Golding and Oertel, 1997). In this study, we primarily tested stimulus conditions that produced simple sodium spikes, but dendritic calcium transients generated by complex spikes are considerably larger than those produced by simple spikes (Roberts et al., 2008). Conditions that promote complex spiking are therefore likely to produce more prominent endocannabinoid release than observed under our experimental conditions.

Input specificity of spiking-evoked suppression

Although CB1 receptors are located on presynaptic inhibitory inputs to CWCs and can be activated by exogenous CB1 agonists (Tzounopoulos et al., 2007), these synapses do not exhibit DSI (Zhao et al., 2009). Electron microscopic and pharmacological data suggest that the differential sensitivity of excitatory and inhibitory inputs to CWCs may result from lower levels of CB1 expression on presynaptic terminals of inhibitory inputs (Tzounopoulos et al., 2007; Zhao et al., 2009). Consistent with these findings, we observed that CWC firing does not cause suppres-

sion of IPSCs. Endocannabinoid release evoked by elevated CWC firing rates will therefore selectively suppress excitatory but not inhibitory inputs.

Mechanisms influencing CWC firing rates

CWCs fire spontaneously *in vivo* at mean rates of ~10–20 Hz (Ding and Voigt, 1997; Portfors and Roberts, 2007) in mice and gerbils. In our slice recording, tonic endocannabinoid release did not occur at these firing rates. However, endocannabinoid release was evoked when firing rates exceeded ~25–30 Hz for several seconds. Consistent with these observations, the relationship between plateau levels of dendritic calcium and CWC firing rate (Figs. 3*C*, 6*B*) began to climb more steeply above 20 Hz. In future studies, it will be of interest to investigate the possibility that different sources of calcium contribute to endocannabinoid release in response to voltage steps and trains of backpropagating action potentials.

Implications for DCN function

Endocannabinoid release produced by submicromolar calcium elevations suggests that endocannabinoid signaling occurs under physiologically realistic conditions. Mechanisms that elevate CWC firing rates *in vivo* include somatosensory and acoustic stimuli. CWCs respond strongly to activation of brainstem nuclei such as the dorsal column nuclei and spinal trigeminal nucleus that convey information about the head and pinna position (Davis and Young, 1997; Ding and Voigt, 1997; Kanold and Young, 2001). Our data suggest that endocannabinoid release from CWCs occurs in response to modest elevations of CWC firing rates for several seconds, and may therefore occur in response to a wide range of stimuli that activate PFs.

In vivo studies have shown that somatosensory inputs that activate the PF pathway provide strong suppression of fusiform cells that provide the main output of the DCN (Davis et al., 1996; Davis and Young, 1997; Kanold and Young, 2001; Koehler et al., 2011). This suppression results from feedforward inhibition of fusiform cells by CWCs. By suppressing PF strength, endocannabinoids released by CWCs can regulate the strength of this feedforward inhibition. Recent studies indicate that PFs make sparse contacts among neighboring CWCs and fusiform cells, whereas CWCs have a high probability of contacting their neighbors (Mancilla and Manis, 2009; Roberts and Trussell, 2010). PFs that exhibit periods of high activity will therefore elevate CWC firing, producing lateral inhibition among the CWC network and suppressing fusiform cell output. Because of the sparseness of PF innervation of neighboring CWCs, less active PF synapses onto a particular CWC can become suppressed but still retain their ability to activate other CWCs.

In addition to spike-timing-dependent long-term plasticity mediated by endocannabinoid release from CWCs (Tzounopoulos et al., 2007), retrograde signaling by endocannabinoids at PF–CWC synapses may also provide a physiological mechanism for short-term plasticity of PF synapses. We find that PF activity can elevate CWC firing rates and evoke release of endocannabinoids, as revealed by monitoring synaptic responses in an independent group of PF inputs to the CWC. Despite the release of endocannabinoids from the postsynaptic CWC, the subset of active PF inputs that drive high-frequency CWC activity exhibits PTP, a form of short-term synaptic enhancement that lasts tens of seconds and results from accumulation of presynaptic calcium during repetitive synaptic activity (Zucker and Regehr, 2002). Enhancement of release by PTP can act through an increase in presynaptic calcium influx per action potential (Habets and Borst, 2006), enhancement of the sensitivity of neurotransmitter release to calcium (Korogod et al., 2007), and an increase in the size of the readily releasable pool (Habets and Borst, 2007; Lee et al., 2010). These mechanisms act in opposition to CB1 receptors, which reduce calcium influx into the presynaptic terminal by inhibiting voltage-gated calcium channels (Brown et al., 2004). Presynaptic enhancement caused by PTP may therefore overcome the suppression mediated by CB1 receptor activation under our experimental conditions. Subsets of PF inputs can thus evoke suppression of other inputs in a heterosynaptic manner while remaining potentiated by evoking endocannabinoid release from the postsynaptic CWC. In this way, somatosensory input from one particular source or modality could reduce the ability of inputs from another source to influence the firing rate of a CWC. Activation of as few as three PF synapses is sufficient to significantly elevate spontaneous CWC firing rates (Roberts and Trussell, 2010), suggesting that activity of only a small fraction of the total population of PF inputs to a CWC would be required to elevate firing rates to levels that would evoke endocannabinoid release.

References

Berrebi AS, Morgan JI, Mugnaini E (1990) The Purkinje cell class may extend beyond the cerebellum. J Neurocytol 19:643–654.

Brenowitz SD, Regehr WG (2003) Calcium dependence of retrograde inhibition by endocannabinoids at synapses onto Purkinje cells. J Neurosci 23:6373–6384.

Brenowitz SD, Regehr WG (2005) Associative short-term synaptic plasticity mediated by endocannabinoids. Neuron 45:419–431.

Brenowitz SD, Best AR, Regehr WG (2006) Sustained elevation of dendritic calcium evokes widespread endocannabinoid release and suppression of synapses onto cerebellar Purkinje cells. J Neurosci 26:6841–6850.

Brown SP, Brenowitz SD, Regehr WG (2003) Brief presynaptic bursts evoke synapse-specific retrograde inhibition mediated by endogenous cannabinoids. Nat Neurosci 6:1048–1057.

Brown SP, Safo PK, Regehr WG (2004) Endocannabinoids inhibit transmission at granule cell to Purkinje cell synapses by modulating three types of presynaptic calcium channels. J Neurosci 24:5623–5631.

Chen K, Waller HJ, Godfrey DA (1995) Muscarinic receptor subtypes in rat dorsal cochlear nucleus. Hear Res 89:137–145.

Davis KA, Young ED (1997) Granule cell activation of complex-spiking neurons in dorsal cochlear nucleus. J Neurosci 17:6798–6806.

Davis KA, Young ED (2000) Pharmacological evidence of inhibitory and disinhibitory neuronal circuits in dorsal cochlear nucleus. J Neurophysiol 83:926–940.

Davis KA, Miller RL, Young ED (1996) Effects of somatosensory and parallel-fiber stimulation on neurons in dorsal cochlear nucleus. J Neurophysiol 76:3012–3024.

Ding J, Voigt HF (1997) Intracellular response properties of units in the dorsal cochlear nucleus of unanesthetized decerebrate gerbil. J Neurophysiol 77:2549–2572.

Freund TF, Katona I, Piomelli D (2003) Role of endogenous cannabinoids in synaptic signaling. Physiol Rev 83:1017–1066.

Fujino K, Oertel D (2003) Bidirectional synaptic plasticity in the cerebellum-like mammalian dorsal cochlear nucleus. Proc Natl Acad Sci U S A 100:265–270.

Gao Y, Vasilyev DV, Goncalves MB, Howell FV, Hobbs C, Reisenberg M, Shen R, Zhang MY, Strassle BW, Lu P, Mark L, Piesla MJ, Deng K, Kouranova EV, Ring RH, Whiteside GT, Bates B, Walsh FS, Williams G, Pangalos MN, et al. (2010) Loss of retrograde endocannabinoid signaling and reduced adult neurogenesis in diacylglycerol lipase knock-out mice. J Neurosci 30:2017–2024.

Golding NL, Oertel D (1997) Physiological identification of the targets of cartwheel cells in the dorsal cochlear nucleus. J Neurophysiol 78:248–260.

Grynkiewicz G, Poenie M, Tsien RY (1985) A new generation of Ca^{2+} indicators with greatly improved fluorescence properties. J Biol Chem 260:3440–3450.

Habets RL, Borst JG (2006) An increase in calcium influx contributes to post-tetanic potentiation at the rat calyx of Held synapse. J Neurophysiol 96:2868–2876.

Habets RL, Borst JG (2007) Dynamics of the readily releasable pool during post-tetanic potentiation in the rat calyx of Held synapse. J Physiol 581:467–478.

Kano M, Ohno-Shosaku T, Hashimotodani Y, Uchigashima M, Watanabe M (2009) Endocannabinoid-mediated control of synaptic transmission. Physiol Rev 89:309–380.

Kanold PO, Young ED (2001) Proprioceptive information from the pinna provides somatosensory input to cat dorsal cochlear nucleus. J Neurosci 21:7848–7858.

Kanold PO, Davis KA, Young ED (2011) Somatosensory context alters auditory responses in the cochlear nucleus. J Neurophysiol 105:1063–1070.

Kim Y, Trussell LO (2007) Ion channels generating complex spikes in cartwheel cells of the dorsal cochlear nucleus. J Neurophysiol 97:1705–1725.

Koehler SD, Pradhan S, Manis PB, Shore SE (2011) Somatosensory inputs modify auditory spike timing in dorsal cochlear nucleus principal cells. Eur J Neurosci 33:409–420.

Korogod N, Lou X, Schneggenburger R (2007) Posttetanic potentiation critically depends on an enhanced Ca(2+) sensitivity of vesicle fusion mediated by presynaptic PKC. Proc Natl Acad Sci U S A 104:15923–15928.

Kreitzer AC, Regehr WG (2001) Retrograde inhibition of presynaptic calcium influx by endogenous cannabinoids at excitatory synapses onto Purkinje cells. Neuron 29:717–727.

Lee JS, Ho WK, Lee SH (2010) Post-tetanic increase in the fast-releasing synaptic vesicle pool at the expense of the slowly releasing pool. J Gen Physiol 136:259–272.

Maejima T, Hashimoto K, Yoshida T, Aiba A, Kano M (2001) Presynaptic inhibition caused by retrograde signal from metabotropic glutamate to cannabinoid receptors. Neuron 31:463–475.

Maejima T, Oka S, Hashimotodani Y, Ohno-Shosaku T, Aiba A, Wu D, Waku K, Sugiura T, Kano M (2005) Synaptically driven endocannabinoid release requires Ca^{2+}-assisted metabotropic glutamate receptor subtype 1 to phospholipase Cβ4 signaling cascade in the cerebellum. J Neurosci 25:6826–6835.

Mancilla JG, Manis PB (2009) Two distinct types of inhibition mediated by cartwheel cells in the dorsal cochlear nucleus. J Neurophysiol 102:1287–1295.

Manis PB, Spirou GA, Wright DD, Paydar S, Ryugo DK (1994) Physiology and morphology of complex spiking neurons in the guinea pig dorsal cochlear nucleus. J Comp Neurol 348:261–276.

Molitor SC, Manis PB (1997) Evidence for functional metabotropic glutamate receptors in the dorsal cochlear nucleus. J Neurophysiol 77:1889–1905.

Molitor SC, Manis PB (2003) Dendritic Ca^{2+} transients evoked by action potentials in rat dorsal cochlear nucleus pyramidal and cartwheel neurons. J Neurophysiol 89:2225–2237.

Mugnaini E, Berrebi AS, Dahl AL, Morgan JI (1987) The polypeptide PEP-19 is a marker for Purkinje neurons in cerebellar cortex and cartwheel neurons in the dorsal cochlear nucleus. Arch Ital Biol 126:41–67.

Myoga MH, Beierlein M, Regehr WG (2009) Somatic spikes regulate dendritic signaling in small neurons in the absence of backpropagating action potentials. J Neurosci 29:7803–7814.

Neher E, Augustine GJ (1992) Calcium gradients and buffers in bovine chromaffin cells. J Physiol 450:273–301.

Oertel D, Young ED (2004) What's a cerebellar circuit doing in the auditory system? Trends Neurosci 27:104–110.

Ohno-Shosaku T, Maejima T, Kano M (2001) Endogenous cannabinoids mediate retrograde signals from depolarized postsynaptic neurons to presynaptic terminals. Neuron 29:729–738.

Ohno-Shosaku T, Shosaku J, Tsubokawa H, Kano M (2002) Cooperative endocannabinoid production by neuronal depolarization and group I metabotropic glutamate receptor activation. Eur J Neurosci 15:953–961.

Petralia RS, Wang YX, Zhao HM, Wenthold RJ (1996) Ionotropic and metabotropic glutamate receptors show unique postsynaptic, presynaptic, and glial localizations in the dorsal cochlear nucleus. J Comp Neurol 372:356–383.

Portfors CV, Roberts PD (2007) Temporal and frequency characteristics of cartwheel cells in the dorsal cochlear nucleus of the awake mouse. J Neurophysiol 98:744–756.

Requarth T, Sawtell NB (2011) Neural mechanisms for filtering self-generated sensory signals in cerebellum-like circuits. Curr Opin Neurobiol 21:602–608.

Roberts MT, Trussell LO (2010) Molecular layer inhibitory interneurons provide feedforward and lateral inhibition in the dorsal cochlear nucleus. J Neurophysiol 104:2462–2473.

Roberts MT, Bender KJ, Trussell LO (2008) Fidelity of complex spike-mediated synaptic transmission between inhibitory interneurons. J Neurosci 28:9440–9450.

Schneggenburger R, Zhou Z, Konnerth A, Neher E (1993) Fractional contribution of calcium to the cation current through glutamate receptor channels. Neuron 11:133–143.

Shore SE, Zhou J (2006) Somatosensory influence on the cochlear nucleus and beyond. Hear Res 216–217:90–99.

Shore SE, Vass Z, Wys NL, Altschuler RA (2000) Trigeminal ganglion innervates the auditory brainstem. J Comp Neurol 419:271–285.

Tanimura A, Yamazaki M, Hashimotodani Y, Uchigashima M, Kawata S, Abe M, Kita Y, Hashimoto K, Shimizu T, Watanabe M, Sakimura K, Kano M (2010) The endocannabinoid 2-arachidonoylglycerol produced by diacylglycerol lipase alpha mediates retrograde suppression of synaptic transmission. Neuron 65:320–327.

Tzounopoulos T, Rubio ME, Keen JE, Trussell LO (2007) Coactivation of pre- and postsynaptic signaling mechanisms determines cell-specific spike-timing-dependent plasticity. Neuron 54:291–301.

Varma N, Carlson GC, Ledent C, Alger BE (2001) Metabotropic glutamate receptors drive the endocannabinoid system in hippocampus. J Neurosci 21:RC188.

Wang J, Zucker RS (2001) Photolysis-induced suppression of inhibition in rat hippocampal CA1 pyramidal neurons. J Physiol 533:757–763.

Wilson RI, Nicoll RA (2001) Endogenous cannabinoids mediate retrograde signalling at hippocampal synapses. Nature 410:588–592.

Wilson RI, Nicoll RA (2002) Endocannabinoid signaling in the brain. Science 296:678–682.

Wright DD, Ryugo DK (1996) Mossy fiber projections from the cuneate nucleus to the cochlear nucleus in the rat. J Comp Neurol 365:159–172.

Wright DD, Blackstone CD, Huganir RL, Ryugo DK (1996) Immunocytochemical localization of the mGluR1 alpha metabotropic glutamate receptor in the dorsal cochlear nucleus. J Comp Neurol 364:729–745.

Yasuda R, Nimchinsky EA, Scheuss V, Pologruto TA, Oertner TG, Sabatini BL, Svoboda K (2004) Imaging calcium concentration dynamics in small neuronal compartments. Sci STKE 2004:pl5.

Young ED, Davis KA (2002) Circuitry and function of the dorsal cochlear nucleus. In: Integrative functions in the mammalian auditory pathways (Oertel D, Fay RR, Popper AN, eds), pp 160–206. New York: Springer.

Zhang S, Oertel D (1993) Cartwheel and superficial stellate cells of the dorsal cochlear nucleus of mice: intracellular recordings in slices. J Neurophysiol 69:1384–1397.

Zhao Y, Rubio ME, Tzounopoulos T (2009) Distinct functional and anatomical architecture of the endocannabinoid system in the auditory brainstem. J Neurophysiol 101:2434–2446.

Zhou J, Shore S (2004) Projections from the trigeminal nuclear complex to the cochlear nuclei: a retrograde and anterograde tracing study in the guinea pig. J Neurosci Res 78:901–907.

Zucker RS, Regehr WG (2002) Short-term synaptic plasticity. Annu Rev Physiol 64:355–405.